Bioorganic & Medicinal Chemistry Letters 20 (2010) 828–831

Contents lists available at ScienceDirect

Bioorganic & Medicinal Chemistry Letters

journal homepage: www.elsevier.com/locate/bmcl

Design and synthesis of piperazine-indole p38α MAP kinase inhibitors with improved pharmacokinetic profiles

Xuefei Tan *, Richland W. Tester, Gregory R. Luedtke, Sarvajit Chakravarty, Babu J. Mavunkel, John J. Perumattam, Qing Lu, Imad Nashashibi, Joon Jung, Jie Hu, Albert Liclican, Ramona Almirez, Jocelyn Tabora, Vinh Tran, Maureen Laney, Daniel E. Levy *, Sundeep Dugar

Department of Medicinal Chemistry and Biology, Scios inc., 6500 Paseo Padre Parkway, Fremont, CA 94555, United States

ARTICLE INFO

Article history:
Received 26 October 2009
Revised 23 December 2009
Accepted 24 December 2009
Available online 4 January 2010

Keywords:
p38
MAP
Kinase
Inhibitor
Inflammatory

ABSTRACT

Derivatives of the 4-fluorobenzyl dimethylpiperazine-indole class of p38α MAP kinase inhibitors are described. Biological evaluation of these compounds focused on maintaining activity while improving pharmacokinetic (PK) properties. Improved properties were observed for structures bearing substitutions on the benzylic methylene.

The effectiveness of modulating pro-inflammatory cytokines in the treatment of diseases including rheumatoid arthritis and psoriasis is demonstrated by the beneficial effects of anti-TNFα therapeutics such as Enbrel and Remicade.[1–4] However, due to disadvantages including high costs and inconvenient dosing regimens, new generations of anti-inflammatory therapies call for the development of safe and effective orally active small molecules. Of particular interest is the development of selective inhibitors of the p38 MAP kinase pathway.[5–7]

The α isoform of p38 MAP kinase has been shown to be a control point which, when activated, leads to the downstream release of a pro-inflammatory cassette of cytokines including interleukin-1β (IL-1β), interleukin-6 (IL-6) and tumor necrosis factor α (TNFα). As p38α activation is not involved in normal physiology, increases in the levels of these cytokines are thought to play a pathophysiological role in inflammatory processes associated with rheumatoid arthritis,[8–10] inflammatory bowel disease,[11] congestive heart failure[12] and psoriasis.[13] Since p38α activation leads to cytokine expression, it is thought that inhibition of p38α with compounds such as SCIO-469 (Fig. 1) can normalize this aberrant physiology and play a key role in the treatment of inflammatory disorders. In fact, SCIO-469 was evaluated in human phase I and phase II clinical trials.[14,15]

SCIO-469 is a potent inhibitor of p38α (IC_{50} = 9 nM), with modest isoform selectivity over p38β (IC_{50} = 98 nM). Furthermore, it is over 1000-fold selective against a number of additional kinases and receptors. The compound inhibits LPS-induced cytokine release in human peripheral blood mononuclear cells (PBMCs) (EC_{50} = 20–50 nM for TNFα, IL-1β, IL-6, IL-8) and blocks the LPS-induced release of TNFα in 10× diluted human whole blood (EC_{50} = 300 nM). It has oral bioavailability in rat (*F*% 15), dog (*F*% 69), and monkey (*F*% 12) with a dose-dependent linear PK profile and is active in a rat collagen induced arthritis model at 40 mg/kg, QD. Unfortunately, the half life ($T_{1/2}$) of SCIO-469 is relatively short as revealed in various animal PK evaluations. In fact, from both in vitro and in vivo metabolism studies, a major debenzylated metabolite (**1**) was observed and was thought to be responsible for the shortened half life (Fig. 2). Due to these problems, considerable effort was placed on the development of next-generation backups with improved pharmacokinetic profiles compared to SCIO-469.

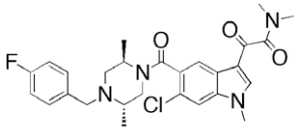

SCIO-469
p38α IC_{50} 0.009 mM

Figure 1. Structure and p38α enzymatic potency of SCIO-469.

* Corresponding authors. Tel.: +11 86 22 66282937 (X.T.); +1 650 704 3051 (D.E.L.).
E-mail addresses: Xuefei827@gmail.com (X. Tan), del345@gmail.com (D.E. Levy).

0960-894X/$ - see front matter © 2009 Elsevier Ltd. All rights reserved.
doi:10.1016/j.bmcl.2009.12.091

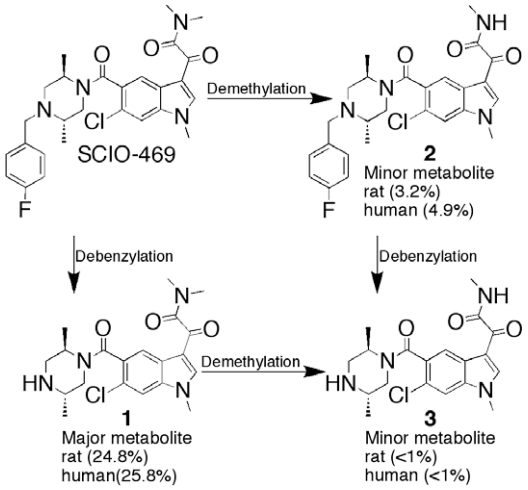

Figure 2. Major metabolites of SCIO-469 identified from liver microsomal incubation.

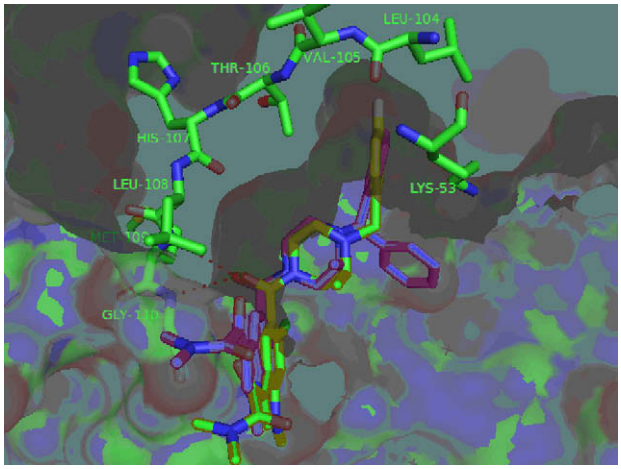

Figure 3. Proposed binding of SCIO-469 (yellow) and compound **9** (magenta) to p38α using a published p38α X-ray crystal structure (PDB code: 1ove). Carbonyl oxygen of SCIO-469 and **9** make bi-dentate hydrogen bonds to backbone nitrogen of Met-109 and Gly-100. 4-Fluoro benzyl group of SCIO-469 and one of the phenyl rings of the diphenylmethane analog of **9** occupy a hydrophobic pocket commonly known as the gatekeeper pocket. In addition, the substituted indole moieties occupy a second hydrophobic pocket near the solvent front. The second phenyl ring of the bis-phenyl moiety of **9** occupies an opening near the conserved residues Lys-53 and Asp-168.

Docking studies of SCIO-469 into a p38α MAP kinase crystal structure revealed additional space at the benzylic position for further substitution (Fig. 3). In an effort to improve the metabolic stability of SCIO-469, introduction of steric bulk at and around the site of metabolism was pursued. Thus, the introduction of methyl, cyano, and phenyl groups at the SCIO-469 benzylic position, as well as the preparation of cyclic compounds (**7**–**12** and **19**) were proposed.

The common intermediate **6**, used in the preparation of compounds **7**–**12**, was prepared from the D-tartaric acid salt of chiral 2,5-dimethyl-4-fluorobenzyl piperazine, compound **4**.[16] As shown in Scheme 1, Boc-protection of compound **4** followed by debenzylation afforded Boc-protected piperazine **5**. Subsequent coupling with 6-chloro-indole carboxylic acid yielded compound **6**. Compounds **7**–**9** were completed by initial treatment of compound **6** with appropriate substituted benzyl bromides followed by reacting with oxalyl chloride and dimethylamine. Compound **10** was prepared similarly but employed a reductive amination instead of a direct displacement. Compounds **11** and **12** were prepared by initial reaction with 4-fluorobenzaldehyde and ethyl aluminum cyanide.[17]

As illustrated in Scheme 2, the synthesis of cyclized indazole analog **19** originated from commercially available *ortho*-chloro

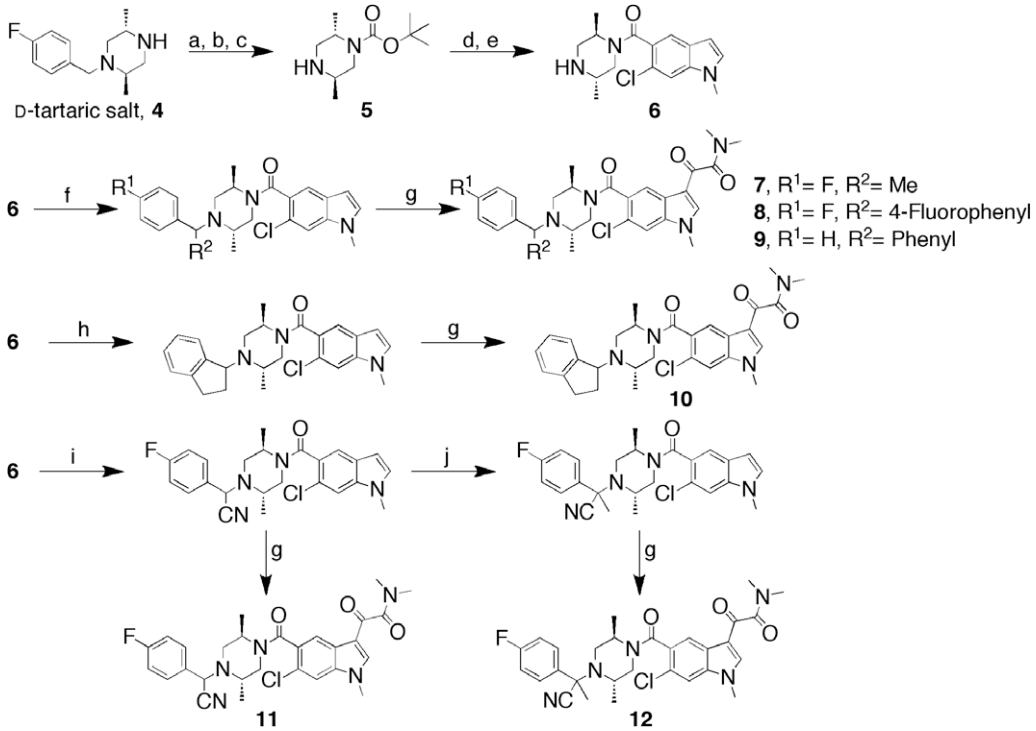

Scheme 1. Reagents and conditions: (a) 10% NaOH, EtOAc 100%; (b) $(Boc)_2O$, Na_2CO_3, dioxane, 46%; (c) $Pd(OH)_2/C$, MeOH, AcOH, H_2, 30 psi, 100%; (d) EDCI, 6-chloro-1-methyl-1*H*-indole-5-carboxylic acid,[16] DMF, Et_3N, 86%; (e) HCl, dioxane, 98%; (f) bromide/ethanol, Et_3N, 66–90%; (g) oxalyl chloride, DCM then dimethyl amine, 74–93%; (h) indan-1-one, $Ti(O\text{-}^iPr)_4$, $NaBH_3CN$, 48%; (i) 4-fluoro-benzaldehyde, $Ti(O\text{-}^iPr)_4$, EtAlCN,[17] 53%; (j) KHMDS, THF then CH_3I, 65%.

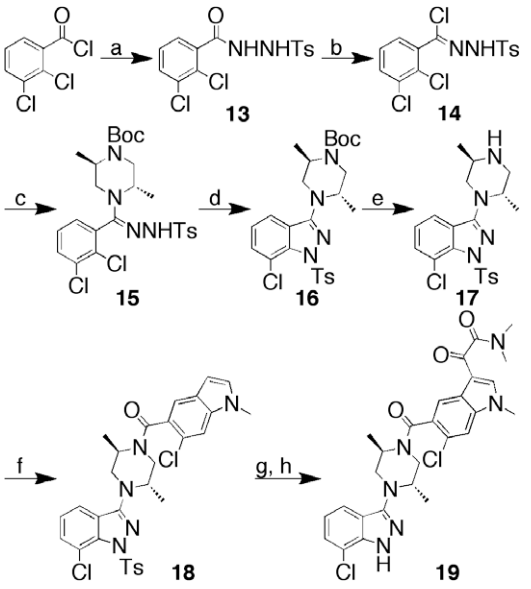

Scheme 2. Reagents and conditions: (a) $TsNHNH_2$, toluene, 97%; (b) $SOCl_2$, 100%; (c) (2*R*,5*S*)-dimethyl-piperazine-1-carboxylic acid *tert*-butyl ester,[18] THF, rt, 65%; (d) K_2CO_3, NMP, 57%; (e) TFA, DCM, 96%; (f) 6-chloro-1-methyl-1*H*-indole-5-carboxylic acid,[16] HATU, Et_3N, DMF, 87%; (g) oxalyl chloride, DCM then dimethyl amine, 83%; (h) KOH, MeOH–H_2O, 90%.

Table 1
Potency and metabolism comparison of SCIO-469 and new analogs

Compds	p38α IC_{50}[19] (μM)	dWBA IC_{50}[20] (μM)	Debenzylated metabolite[a] (%)
SCIO-469	0.009	0.1–0.2	24.8
7	0.006	ND	29.6
8	0.024	24%@0.5 μM[b]	ND
9	0.009	0.5	5.1
10	0.029	0.5	40.8
11	0.183	32%@0.3 μM[b]	Not stable[c]
12	0.047	0.3	Not stable[c]
19	0.048	0.47	<5%

[a] Values are based on MS signal intensity.
[b] Percentage of TNFα inhibition at certain inhibitor concentration.
[c] Significant loss of cyano group was observed in microsomal incubation.

benzoyl chloride. Reaction with tosyl hydrazide followed by treatment with thionyl chloride yielded the chloroimine **14**. Displacement of **14** with (2*R*,5*S*)-dimethyl-piperazine-1-carboxylic acid *tert*-butyl ester[18] provided intermediate **15**, which upon treatment with K_2CO_3, cyclized into indazole **16**. Following the removal of the Boc protecting group, the amine was coupled with 6-chloro-1-methyl-1*H*-indole-5-carboxylic acid[16] to afford compound **18**. Subsequent treatment of **18** with oxalyl chloride and dimethyl amine followed by cleavage of the tosyl protecting group gave the desired indazole analog **19**.

Table 3
In vivo PK profiles of diphenylmethane analog **9**

Species	Rat	Dog	Monkey
CL (L/h/kg)	1.2	0.2	–
V (L/kg)	2.7	6.5	–
C_{max} (ng/mL)	367	899	360
T_{max} (h)	1.2	1.3	2
AUC_{IV} (μg*h/L)	810	3430	–
AUC_{PO} (μg*h/L)	1272	5609	1829
%*F*	31	33	–

As indicated in Table 1, the p38α activity for all, but one of the analogs was below 50 nM, indicating that the predictive model was an effective tool in the design of potent p38α inhibitors. However, the cellular activities (dWBA IC_{50}) of these analogs were clearly dependent upon a compound's cell permeability and not predictive based on modeling. Interestingly, both a more hydrophobic analog **8** and a more polar analog **11** gave the worst cellular activities. The microsomal incubation study shows that only the diphenylmethane analog **9** and indazole analog **19** gave significantly lower levels of the debenzylated metabolite while maintaining potency. Analogs **7** and **10** yielded higher percentages of the debenzylated metabolite whereas **11** and **12** were much less stable under the microsomal incubation conditions. Finally, while microsomal digestion of analog **19**, produced less than 5% of the corresponding debenzylated metabolite, its oral availability (determined in rat PK studies) was found to be much lower than expected. As this compound is structurally quite different than SCIO-469, its poor PK may be due to other factors.

Further microsomal studies of the diphenylmethane analog **9** demonstrate that it is, in fact, more metabolically stable that SCIO-469. Additionally, this trend was observed in multiple species. While it was observed that metabolism of **9** also occurs at the dimethyl amide region of the molecule, a higher percentage of demethylated metabolite, compared to SCIO-469, was formed in every species (Table 2).

Evaluation of compound **9** in in vivo PK studies indicated it has a bioavailability of 31% in rat and 33% in dog. Furthermore, PK parameters such as oral exposure, clearance and volume of distribution, measured in multiple species (Table 3), warranted consideration of compound **9** as a backup to SCIO-469. While lower exposure was observed in monkey, this was consistent with the increased amount of demethylated metabolite noted in the in vitro studies mentioned above.

In summary, through efforts to discover backup molecules with improved pharmacokinetic profiles over SCIO-469, we identified the diphenylmethane group as a superior alternative to the 4-fluorobenzyl moiety in the indole-piperazine class of p38α MAP kinase inhibitors. This modification resulted in improved in vitro and in vivo pharmacokinetic profiles compared to SCIO-469, presumably due to the sterically hindered environment around the site of metabolism. Furthermore, this steric hindrance suppressed the formation of a potential major metabolite while maintaining overall biological properties and potency against p38α MAP kinase.

Table 2
Microsomal metabolism of diphenylmethane analog **9** and SCIO-469 in various species

Microsomal metabolism	Parent[a](%)		Debenzylated metabolite (%)		Demethylated metabolite (%)	
Compds	SCIO-469	**9**	SCIO-469	**9**	SCIO-469	**9**
Rat	65.8	83.9	24.8	5.1	3.2	9.4
Dog	94.5	91.7	2.6	2.5	2.3	4.8
Monkey	51.2	71.4	25.2	2.9	11.9	19.5
Human	65.1	90.8	25.8	1.1	4.9	6.3

[a] Values are based on MS signal intensity.

References and notes

1. Jarvis, B.; Faulds, D. *Drugs* **1999**, *57*, 945.
2. Moreland, L. W.; Schiff, M. H.; Baumgartner, S. W.; Tindall, E. A.; Fleischmann, R. M.; Bulpitt, K. J.; Weaver, A. L.; Keystone, E. C.; Furst, D. E.; Mease, P. J.; Ruderman, E. M.; Horwitz, D. A.; Arkfeld, D. G.; Garrison, L.; Burge, D. J.; Blosch, C. M.; Lange, M. L. M.; McDonnell, N. D.; Weinblatt, M. E. *Ann. Intern. Med.* **1999**, *130*, 478.
3. Choy, E. H.; Panayi, G. S. N. *Eng. J. Med.* **2001**, *344*, 907.
4. Markham, A.; Lamb, H. M. *Drugs* **2000**, *59*, 1341.
5. Lee, J. C.; Laydon, J. T.; McDonnell, P. C.; Gallagher, T. F.; Kumar, S.; Green, D.; McNutly, D.; Blumenthal, M. J.; Heyes, J. R.; Landvatter, S. W.; Strickler, J. E.; McLaughlin, M. M.; Siemens, I. R.; Fisher, S. M.; Livi, G. P.; White, J. R.; Adams, J. L.; Young, P. R. *Nature* **1994**, *372*, 739.
6. Kumar, S.; Boehm, J.; Lee, J. C. *Nat. Rev. Drug Disc.* **2003**, *2*, 717.
7. Saklatvala, J. *Curr. Opin. Pharmacol.* **2004**, *4*, 372.
8. Foster, M. L.; Halley, F.; Souness, J. E. *Drug News Perspect.* **2000**, *13*, 488.
9. Pargellis, C.; Regan, J. *Curr. Opin. Invest. Drugs* **2003**, *4*, 566.
10. Smith, R. J. *Drug Discovery Today* **2005**, *10*, 1598.
11. Badger, A. M.; Bradbeer, J. N.; Votta, B.; Lee, J. C.; Adams, J. L.; Griswold, G. E. *J. Pharmacol. Exp. Ther.* **1996**, *279*, 1453.
12. Kubota, T.; Miyagishima, M.; Alvarez, R. J.; Kormos, R.; Rosenblum, W. D.; Demetris, A. J.; Semigran, M. J.; Dec, G. W.; Holubkov, R.; McTiernan, C. F.; Mann, D. L.; Feldman, A. M.; McNamara, D. M. *J. Heart Lung Transplant.* **2000**, *19*, 819.
13. Sticherling, M. *Drug Discovery Today: Disease Mech.* **2005**, *2*, 275.
14. http://www.accessmylibrary.com/article-1G1-70735265/scios-begin-phase-ib.html.
15. http://clinicaltrials.gov/ct2/show/NCT00089921.
16. Mavunkel, B. J.; Chakravarty, S.; Perumattam, J. J.; Dugar, S.; Lu, Q.; Liang, X. WO 2000/071535, 2000 ((D)-tartaric acid was used in the chiral resolution to obtain (2*S*,5*R*)-2,5-dimethyl-4-fluoro-benzyl piperazine tartaric salt).
17. Baroudy, B. M.; Clader, J. W.; Josien, H. B.; Mccombie, S. W.; Mckittrick, B. A.; Miller, M. W.; Neustadt, B. R.; Palani, A.; Smith, E. M.; Steensma, R.; Tagat, J. R.; Vice, S. F.; Laughlin, M. A.; Gilbert, E.; Labroli, M. A. WO 2000/066558, 2000.
18. (2*R*,5*S*)-Dimethyl-piperazine-1-carboxylic acid *tert*-butyl ester was synthesized using same procedure as for the synthesis of intermediate **5**, except (L)-tartaric salt of chiral (2*S*,5*R*)-2,5-dimethyl-4-fluorobenzyl piperazine was used.
19. Mavunkel, B. J.; Perumattam, J. J.; Tan, X.; Luedtke, G. R.; Lu, Q.; Lim, D.; Kizer, D.; Dugar, S.; Chakravarty, S.; Xu, Y.-j.; Jung, J.; Liclican, A.; Levy, D. E.; Tabora, J. *Bioorg. Med. Chem. Lett.*, in press. doi:10.1016/j.bmcl.2009.12.031.
20. The LPS/TNFα Human Whole Blood Assay was run as described in: Mavunkel, B.; Dugar, S.; Luedtke, G.; Tan, X.; McEnroe, G. US Patent 6,696,443, 2004.